

# Ir<sub>3</sub>Co<sub>6</sub> and Co<sub>3</sub>Fe<sub>3</sub> Dithiolene Cluster Complexes: Multiple Metal–Metal Bond Formation and Correlation between Structure and Internuclear Electronic Communication

Satoru Tsukada,<sup>†</sup> Yusuke Shibata,<sup>†</sup> Ryota Sakamoto,<sup>†</sup> Tetsuya Kambe,<sup>†</sup> Tomoji Ozeki,<sup>‡</sup> and Hiroshi Nishihara<sup>\*,†</sup>

<sup>†</sup>Department of Chemistry, Graduate School of Science, The University of Tokyo, 7-3-1 Hongo, Bunkyo-ku, Tokyo 113-0033, Japan

<sup>‡</sup>Department of Chemistry and Materials Science, Tokyo Institute of Technology, 2-12-1 O-okayama, Meguro-ku, Tokyo 152-8551, Japan

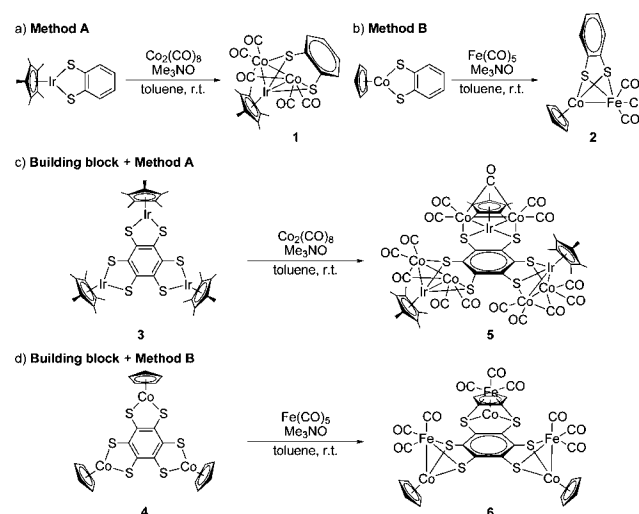
## Supporting Information

**ABSTRACT:**  $\pi$ -Conjugated trinuclear iridium and cobalt dithiolenes undergo multiple metal–metal bond formation with Co<sub>2</sub>(CO)<sub>8</sub> and Fe(CO)<sub>5</sub>, giving rise to Ir<sub>3</sub>Co<sub>6</sub> nonanuclear and Co<sub>3</sub>Fe<sub>3</sub> hexanuclear cluster complexes **5** and **6**, respectively. **5** retains a planar framework and intense  $\pi$  conjugation across the three iridadithiolenes and the phenylene bridge, which results in intense electronic communication among the three Co<sub>2</sub>(CO)<sub>5</sub> units in reduced mixed-valent states.

An important feature of metalladithiolenes is the quasi-aromaticity of the metal-containing five-membered ring.<sup>1</sup> The peculiar electronic structure can stabilize a 16e<sup>-</sup> unsaturated coordination state at the metal center. This electron deficiency proved to be advantageous in an investigation of multinucleation of metalladithiolenes.<sup>2–4</sup> A major portion of this work exploited metal–metal bond formation reactions with low-valent metal molecules;<sup>2,3</sup> for example, we<sup>3</sup> and Jin et al.<sup>5</sup> independently synthesized neutral trinuclear MCo<sub>2</sub> metalladithiolene clusters (M = Rh<sup>3+</sup>, Ir<sup>3+</sup>, Ru<sup>2+</sup>): The synthetic procedure for preparing the IrCo<sub>2</sub> cluster **1** is illustrated in Scheme 1a (method A). The main feature of this metal integration methodology was that the planarity of the metalladithiolene ring was retained, which preserved its quasi-aromaticity.<sup>3a</sup> On the other hand, a reaction of CpCo(S<sub>2</sub>C<sub>6</sub>H<sub>4</sub>) with Fe(CO)<sub>5</sub> produced a dinuclear CoFe cluster complex **2** (Method B, Scheme 1b),<sup>2b</sup> in which the metalladithiolene ring was bent, leading to a loss of the quasi-aromaticity.<sup>2</sup>

Another approach to the multinucleation of metalladithiolenes has used hexamercaptobenzene as a source of dithiolato ligands, which enables the fabrication of trinuclear metalladithiolene complexes featuring highly developed  $\pi$  conjugation.<sup>4</sup> The  $\pi$ -conjugated system in this series of complexes containing group 8–10 metals, such as **3** and **4** (Building Blocks, Scheme 1c,d), displayed intense electronic communication among the three dithiolene units in mixed-valent (MV) states. These findings stimulated a further question: Could the  $\pi$ -conjugated trinuclear dithiolene framework provide MV interactions among other redox-active sites? Given the background elaborated above, here we describe the fabrication of neutral nonanuclear and hexanuclear dithiolene cluster

## Scheme 1. Multinucleation Methodologies for Metalladithiolenes



complexes **5** and **6** (Scheme 1c,d) in combination with the Building Blocks using Methods A and B, respectively. We disclose the single-crystal X-ray structures of **5** and **6** and focus on how altering the planarity of the trinuclear metalladithiolene backbone via metal–metal bond formation influences internuclear electronic communication in reduced MV states.

Two potential structural isomers have syn and anti configurations, where the three [Co<sub>2</sub>] or [Fe] units all trend in the same direction and one of them faces away from the rest, respectively ([Co<sub>2</sub>] = Co<sub>2</sub>(CO)<sub>5</sub> and [Fe] = Fe(CO)<sub>3</sub>). The configurations were successfully identified by single-crystal X-ray structure analysis. **5** exclusively showed the anti structure (Figure 1a and Tables S1 and S2 in the Supporting Information, SI). The methyl groups on the Cp rings were split by a ratio of 2:1 in the <sup>1</sup>H NMR spectrum in chloroform-*d*<sub>1</sub> (Figure S1 in the SI), which also assured the anti configuration in solution. The absence of the syn isomer might be attributed to steric hindrance among the bulky [Co<sub>2</sub>] units. The Co–Ir distances (average: 2.610 Å) were nearly

Received: November 25, 2011

Published: January 26, 2012

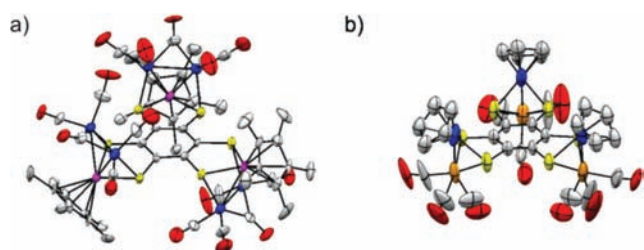


**Figure 1.** ORTEP drawings of (a) **5** and (b) **6** with thermal ellipsoids at the 50% probability level. Hydrogen atoms and crystal solvents are omitted for clarity. Color code: white, C; red, O; yellow, S; blue, Co; magenta, Ir; orange, Fe.

identical with those of Co–Ir bonds in other cluster complexes.<sup>3a,6</sup> Therefore, **5** included direct Co–Ir bonds. The interatomic distances between Co and S were short enough to permit direct bond formation. On the other hand, the Co–C distances were too large to possess direct bonds (Table S2 in the SI). These features indicated that the [Co<sub>2</sub>] units were appended in an η<sup>3</sup>-coordination fashion with one iridium and two sulfur atoms. The plane comprising the three iridadithiolene rings and the central phenylene bridge was slightly bent to form a bowl-like framework, but the extent of the bending was insignificant (the average S–C–C–S torsion angle was 5.72°). The shorter C–C bonds of the central phenylene belonged to the metalladithiolene five-membered rings, whereas the longer ones linked the rings together. The maximum difference among the C–C bond lengths was less than 0.06 Å [shortest, 1.36(2) Å; longest, 1.42(2) Å]. This difference was smaller than that of **3** (0.12 Å),<sup>4b</sup> indicating that the central phenylene of **5** was more strongly aromatic than that of **3**. In total, π conjugation in **5**, which spanned the three iridadithiolene rings and the phenylene bridge, was expected to remain, even upon attachment of the [Co<sub>2</sub>] units.

On the other hand, single-crystal X-ray structure analysis of **6** clarified the syn structure (Figures 1b and S12 in the SI). The protons on the Cp rings were all equivalent in a <sup>1</sup>H NMR spectrum, which ensured the syn structure in solution. The Co–Fe distance in the crystal structure of **6** was 2.381 Å. This was nearly identical with other cluster complexes with direct Co–Fe bonds,<sup>2b,7</sup> indicating that the CpCo moiety and [Fe] unit were connected by a single Co–Fe bond. The sulfur atoms of the benzenhexathiolato ligand constructed coordination bonds with both cobalt and iron (average bond distances: Co–S, 2.306 Å; Fe–S, 2.190 Å). On the other hand, the Co–C (average: 3.169 Å) and Fe–C distances (average: 3.115 Å) were too large to possess direct bonds. The dihedral angles between the benzenhexathiolato ligand and the S–Co–S and S–Fe–S planes were 48.69° and 40.66°, respectively. Through incorporation of the [Fe] units, the planarity of the CoS<sub>2</sub>C<sub>2</sub> rings was lost (Figure S12 in the SI), which also occurred in the previously described cluster complex **2**.<sup>2b</sup>

Figure 2 shows the representative frontier orbitals of **5** and **6** estimated by density functional theory (DFT) calculations; see Figures S4 and S11 in the SI for the rest of the orbitals. In **5**, LUMO to LUMO+2 were mainly based on the [Co<sub>2</sub>] units, with contributions from the iridium and sulfur atoms (Figures 2a and S4 in the SI). This agreed with the study of **1**,<sup>3a</sup> and assured that reductions in **5** initially occurred at the [Co<sub>2</sub>] units. Above these three orbitals lay iridadithiolene(π\*) orbitals (LUMO+3 to LUMO+5; Figure S4 in the SI), to which the iridium atoms provided the greatest contribution. On the other

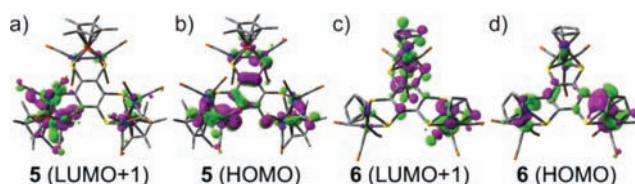


**Figure 2.** Representative frontier orbitals of **5** and **6** estimated by DFT calculations.

hand, HOMO–2 to HOMO contributed to the iridadithiolene(π) orbitals (Figures 2b and S4 in the SI). Here, the sulfur and carbon atoms contributed more electron density than iridium.

LUMO to LUMO+2 of **6** chiefly originated from the [Fe] units (Figures 2c and S11 in the SI): Therefore, the reduction should initially occur at the [Fe] units. LUMO+3 to LUMO+5 mainly stemmed from the cobalt ions, with small contributions from carbon and sulfur atoms comprising the dithiolene ring (Figure S11 in the SI). On the other hand, HOMO–2 to HOMO of **6** were based on both [Fe] units and cobalt ions (Figures 2d and S11 in the SI) by DFT calculations. This result contrasted sharply with the case of **5**, in which iridadithiolene(π) orbitals played a central role in HOMO–2 to HOMO (Figures 2b and S4) and could be rationalized by the fact that the π system comprising the cobaltadithiolenes in **6** was disrupted by the bent structure.

Differential pulse voltammetry of **5** and **6** with respect to reductions was carried out (Figure S5 in the SI), and the numerical data are collected in Table 1, along with the data for

**Table 1.** Electrochemical Data and Comproportionation Constant

	potential/V vs ferrocenium/ferrocene			comproportionation constant	
	$E^{\circ}(\text{X}^{2-}/\text{X}^{3-})$	$E^{\circ}(\text{X}^{2-}/\text{X}^{2-})$	$E^{\circ}(\text{X}/\text{X}^{\cdot-})$	$\log K_c(\text{X}^{2-})$	$\log K_c(\text{X}^{\cdot-})$
<b>5</b> <sup>a</sup>	–1.57	–1.38	–1.22	3.2	2.7
<b>1</b> <sup>b</sup>			–1.27		
<b>6</b> <sup>c</sup>	–1.20	–1.20	–1.06	0.0	2.4
<b>2</b> <sup>d</sup>			–1.48		

<sup>a</sup>In 0.1 M Bu<sub>4</sub>NClO<sub>4</sub><sup>–</sup>PhCN. <sup>b</sup>In 0.1 M Bu<sub>4</sub>NClO<sub>4</sub><sup>–</sup>CH<sub>3</sub>CN. Reference 3a. <sup>c</sup>In 0.1 M Bu<sub>4</sub>NClO<sub>4</sub><sup>–</sup>PhCN/toluene (1:1 v/v). <sup>d</sup>In 0.1 M Bu<sub>4</sub>NClO<sub>4</sub><sup>–</sup>CH<sub>3</sub>CN. Reference 2b.

the related compounds **1** and **2**. **5** underwent three reversible one-electron reductions. Judging from the DFT calculations (Figures 2a,b and S4 in the SI), these redox waves could be assigned to electron donation to the three [Co<sub>2</sub>] units. These three reductions in **5** occurred in a stepwise fashion, and these splits were assigned to electronic communication in the MV states. The comproportionation constant,  $K_c$ , which is one of the most convenient indicators of electronic communication, is defined as follows:<sup>8</sup>

$$K_c(\text{X}^-) = \frac{[\text{X}^-]^2}{[\text{X}][\text{X}^{2-}]} = \exp\{[E^{\circ}(\text{X}^-/\text{X}^-) - E^{\circ}(\text{X}^-/\text{X}^{2-})]F/RT\} \quad (1)$$

$$K_c(\text{X}^{2-}) = \frac{[\text{X}^{2-}]^2}{[\text{X}^-][\text{X}^{3-}]} = \exp\{[E^{\circ}(\text{X}^-/\text{X}^{2-}) - E^{\circ}(\text{X}^{2-}/\text{X}^{3-})]F/RT\} \quad (2)$$

where  $[\text{X}^{n-}]$  is the concentration of the chemical species  $\text{X}^{n-}$  and  $E^{\circ}(\text{X}^{n-}/\text{X}^{(n-1)-})$  is the formal potential of the  $\text{X}^{n-}/\text{X}^{(n-1)-}$  redox couple. The  $\log K_c(\text{5}^-)$  and  $\log K_c(\text{5}^{2-})$  values are

tabulated in Table 1. **5** yielded large values of  $\log K_c$ , even in 0.1 M NaBPh<sub>4</sub>/THF (Figure S6 and Table S3 in the SI), in which strong ion-pairing effects were present, and the Coulombic contribution to  $K_c$  was consequently reduced.<sup>9a,b</sup> This assured that the contribution of electronic communication dominated the large  $K_c$  of **5**. Astruc and co-workers have reported a contrastive molecular system that features no electronic communication among redox sites: In this system, the splits of the formal potentials of the redox sites have diminished in electrolyte solution with a strong ion-pairing ability.<sup>9c</sup> We note that the anti [Co<sub>2</sub>] unit experienced a chemical environment different from that of the other two counterparts, which could induce heterogeneous formal potentials. In the case of **5**, however, the heterogeneity was expected to be trivial: The platform for the [Co<sub>2</sub>] units, **4**, featured pseudo-*D*<sub>3h</sub> symmetry. Therefore, the [Co<sub>2</sub>] units received the same bonding fashion and experienced a similar extent of electronic communication, irrespective of the direction of the bond formation. A similar discussion had been applied toward the phenylene-annulated ferrocenyl trimer, in which electronic communication was observed, even in the anti isomer.<sup>10</sup> On the other hand, splits in the formal potentials upon reductions of **6** were less prominent than those of **5** (Figure S5b in the SI), even in less polar media, for example, a mixture of toluene and PhCN, which could enhance the Coulombic contribution. Considering the DFT calculations (Figures 2 and S4 and S11 in the SI), a plausible mechanism for electronic communication in **5** and **6** was electron superexchange via vacant orbitals or iridium or cobalt metalladithiolene  $\pi^*$  orbitals (LUMO+3 to LUMO+5). This mechanism could well explain the experimental fact that **6** displayed weaker electronic communication because the  $\pi^*$  orbitals were disrupted in **6** by the structural distortion, as observed in the X-ray structure (Figure 1b).

In conclusion, we synthesized nonanuclear Ir<sub>3</sub>Co<sub>6</sub> and hexanuclear Co<sub>3</sub>Fe<sub>3</sub> dithiolene metal cluster complexes **5** and **6** by means of our multinucleation methodologies applied to the  $\pi$ -conjugated trinuclear metalladithiolenes. **5** and **6** featured Co–Ir and Fe–Co metal–metal bonds, although the planar framework of the phenylene-bridged three metalladithiolenes was retained only in **5**. This planar configuration and the resultant  $\pi$ -conjugated electronic structure yielded strong electronic communication in the reduced MV states among the three [Co<sub>2</sub>] units in **5**. In sharp contrast, **6** displayed a far weaker interaction among the [Fe] units because of the bent metalladithiolene rings and the accompanying disrupted  $\pi$  conjugation. Our methodology to build up gigantic multinuclear heterometal cluster complexes can contribute to one of the immature regions of chemistry: precise syntheses of metal-containing molecules. Also, this strategy involving the expression of distant electronic communication, utilization of  $\pi$ -conjugated metal complex bridges and metal–metal bond formation, and its controllability via structural changes in the bridge has provided new insight into MV chemistry.

## ■ ASSOCIATED CONTENT

### ■ Supporting Information

Experimental details, crystallographic data of **5** and **6** (Tables S1, S2 and S4), <sup>1</sup>H NMR spectrum of **5** (Figure S1), IR spectra of **5** and **6** (Figures S2 and S8), XPS of **5** and **6** (Figures S3 and S9), DFT calculations (Figures S4 and S11), cyclic voltammograms of **5** (Figures S5 and S6 and Table S3), and UV–vis spectra of **5** and **6** (Figures S7 and S10). This material is available free of charge via the Internet at <http://pubs.acs.org>.

## ■ AUTHOR INFORMATION

### Corresponding Author

\*E-mail: [nishihara@chem.s.u-tokyo.ac.jp](mailto:nishihara@chem.s.u-tokyo.ac.jp)

### Notes

The authors declare no competing financial interest.

## ■ ACKNOWLEDGMENTS

The authors acknowledge Grants-in-Aid from MEXT of Japan (Grants 20245013 and 21108002, area 2107), a JSPS Research Fellowship for Young Scientists, and the Global COE Program for Chemistry Innovation for financial support.

## ■ REFERENCES

- (1) (a) Stiefel, E. L., Ed. *Dithiolene Chemistry; Synthesis, Properties, and Applications. Progress in Inorganic Chemistry*; Wiley: Hoboken, NJ, 2004; Vol. 52. (b) Eisenberg, R. *Prog. Inorg. Chem.* **1970**, *12*, 295–369. (c) Burns, R. P.; McAullife, C. A. *Adv. Inorg. Chem. Radiochem.* **1979**, *22*, 303–348. (d) Fourmigue, M. *Coord. Chem. Rev.* **1998**, *178–180*, 823–864. (e) Sugimori, A.; Akiyama, T.; Kajitani, M.; Sugiyama, T. *Bull. Chem. Soc. Jpn.* **1999**, *72*, 879–908. (f) Liu, S.; Han, Y.-F.; Jin, G.-X. *Chem. Soc. Rev.* **2007**, *36*, 1543–1560. (g) Meng, X.; Wang, F.; Jin, G.-X. *Coord. Chem. Rev.* **2010**, *254*, 1260–1272.
- (2) (a) Nihei, M.; Nankawa, T.; Kurihara, M.; Nishihara, H. *Angew. Chem., Int. Ed.* **1999**, *38*, 1098–1100. (b) Murata, M.; Habe, S.; Araki, S.; Namiki, K.; Yamada, T.; Nakagawa, N.; Nankawa, T.; Nihei, M.; Mizutani, J.; Kurihara, M.; Nishihara, H. *Inorg. Chem.* **2006**, *45*, 1108–1116. (c) Zhu, B.-H.; Shibata, Y.; Muratsugu, S.; Yamanoi, Y.; Nishihara, H. *Angew. Chem., Int. Ed.* **2009**, *48*, 3858–3861. (d) Muratsugu, S.; Sodeyama, K.; Kitamura, F.; Sugimoto, M.; Tsuneyuki, S.; Miyashita, S.; Kato, T.; Nishihara, H. *J. Am. Chem. Soc.* **2009**, *131*, 1388–1389. (e) Muratsugu, S.; Sodeyama, K.; Kitamura, F.; Tsukada, S.; Tada, M.; Tsuneyuki, S.; Nishihara, H. *Chem. Sci.* **2011**, *2*, 1960–1968.
- (3) (a) Nakagawa, N.; Yamada, T.; Murata, M.; Sugimoto, M.; Nishihara, H. *Inorg. Chem.* **2006**, *45*, 14–16. (b) Nakagawa, N.; Murata, M.; Sugimoto, M.; Nishihara, H. *Eur. J. Inorg. Chem.* **2006**, 2129–2131.
- (4) (a) Nishihara, H.; Okuno, M.; Kogawa, N.; Aramaki, K. *J. Chem. Soc., Dalton Trans.* **1998**, *120*, 2651–2656. (b) Shibata, Y.; Zhu, B.-H.; Kume, S.; Nishihara, H. *Dalton Trans.* **2009**, 1939–1943. (c) Kambe, T.; Tsukada, S.; Sakamoto, R.; Nishihara, H. *Inorg. Chem.* **2011**, *50*, 6856–6858.
- (5) Wang, J.-Q.; Hou, X.; Weng, L.; Jin, G.-X. *Organometallics* **2005**, *24*, 826–830.
- (6) (a) Herrmann, W. A.; Barnes, C. E.; Zahn, T.; Ziegler, M. L. *Organometallics* **1985**, *4*, 172–180. (b) Hörlein, R.; Herrmann, W. A.; Barnes, C. E.; Weber, C.; Krüger, C.; Ziegler, M. L.; Zahn, T. *J. Organomet. Chem.* **1987**, *321*, 257–272. (c) Livotto, F. S.; Vargaa, M. D.; Grepioni, F.; Braga, D. *J. Organomet. Chem.* **1993**, *452*, 197–203. (d) Chen, J.; Daniels, L. M.; Angelici, R. J. *Organometallics* **1996**, *15*, 1223–1229. (e) Chen, J.; Young, V. G.; Angelici, R. J. *Organometallics* **1996**, *15*, 1414–1421.
- (7) (a) Mathur, P.; Sekar, P.; Satyanarayana, C. V. V.; Mahon, M. F. *J. Organomet. Chem.* **1996**, *522*, 291–295. (b) Manning, A. R.; McAdam, C. J.; Palmer, A. J.; Robinson, B. H.; Simpson, J. *Dalton Trans.* **2003**, 4472–4481. (c) Cai, S.; Hou, X.-F.; Chen, Y.-Q.; Jin, G.-X. *Dalton Trans.* **2006**, 3736–3741.
- (8) Creutz, C. *Prog. Inorg. Chem.* **1983**, *30*, 1–73 and references cited therein.
- (9) (a) Barrière, F.; Geiger, W. E. *J. Am. Chem. Soc.* **2006**, *128*, 3980–3989. (b) Geiger, W. E.; Barrière, F. *Acc. Chem. Res.* **2010**, *43*, 1030–1039. (c) Diallo, A. K.; Absalon, C.; Ruiz, J.; Astruc, D. *J. Am. Chem. Soc.* **2011**, *133*, 629–641.
- (10) Santi, S.; Orian, L.; Donoli, A.; Bisello, A.; Scapinello, M.; Benetollo, F.; Ganis, P.; Ceccon, A. *Angew. Chem., Int. Ed.* **2008**, *47*, 5331–5334.